

Taguchi Grey Relational Analysis of Chloride Diffusivity of Mortar Containing Nano-Titanium Dioxide

Yogesh Iyer Murthy

yogesh.murthy@juet.ac.in


Jaypee University of Engineering and Technology

Method Article

Keywords: Chloride Diffusion, Effective diffusivity, Grey Relational Analysis, Nano-Titanium Dioxide

Posted Date: March 7th, 2024

DOI: <https://doi.org/10.21203/rs.3.rs-4013290/v1>

License:  This work is licensed under a Creative Commons Attribution 4.0 International License. [Read Full License](#)

Additional Declarations: No competing interests reported.

Abstract

The present research investigates the usefulness of NT as a filler ingredient and its influence on the reduction of chloride ion diffusivity (D_{eff}) in mortar. The flow of Cl^- ions or flux through the mortar is influenced by the concentration of NT in the material; as NT content increases, flux decreases, indicating a delay in ion migration. There is a negative correlation between the concentration of NT and the diffusion of Cl^- ions in the anolyte chamber; the control specimen demonstrates the greatest diffusion. The sample containing NT exhibits a notably reduced diffusion of Cl^- ions in comparison to the control sample, indicating a decline in the mobility of Cl^- ions in both chambers. Maximum compressive strength of mortar on 3, 7, 28, 56 and 90 days was obtained at 1.5% replacement as also evident from the microstructure at 28 days. The Grey ranking proposed that the control mix has the lowest rank of D_{eff} and decreased with decreasing NT replacement. It is concluded that the Taguchi-based grey relational analysis method is an extremely useful instrument for optimizing such experimental studies. Grey relationship coefficients affect resource utilization, energy efficiency, and cost-effectiveness; hence this study could increase process efficiency.

Introduction

The corrosion of steel in concrete that is caused by chloride is one of the most common factors that contribute to the deterioration of reinforced concrete structures. In particular, the design and construction of structures that will be developed in maritime environments require a distinct evaluation of chloride permeability since it is such an important characteristic that it must be analyzed individually [1]. In addition to capillary suction and absorption, ion diffusion in water is another method by which chlorides are introduced into concrete. This could lead to a significant concentration of chloride ions on the surface of the reinforcing steel if the infiltration process is repeated or carried out over an extended period of time [2]. As the reinforcing steel is subjected to alternating wetting and drying, or freezing and thawing, it becomes increasingly apparent that salts are making their way towards the steel. Due to the fact that the concrete is susceptible to movement and the accumulation of harmful components, the cyclic action makes the durability difficulties even more challenging [2]–[4].

The incorporation of fine fillers has the effect of hastening the hydration process of cement [5]. When fine powders of limestone, quartz, silica fume, and pulverized fly ash are applied at a maximum cement replacement level of 15%, it has been established that the application of fine powders of limestone, quartz, silica fume, and pulverized fly ash can reduce the amount of time it takes for cement to hydrate [6].

Fine fillers, on the other hand, have the potential to influence the dimensional stability of a cement mix by causing the cementitious material to shrink [7], [8]. Researchers observed an increase in chemical shrinkage after the addition of fine fillers to cement paste by the researchers. According to the findings of earlier investigations [9], the addition of "coarse" particles to cement pastes did not reduce the amount of chemical shrinkage that occurred when compared to the addition of OPC mixes. As a consequence of this,

the particle size of the filler that is added to the cement can be optimized in order to hasten the hydration process while having a minor effect on the dimensional stability of the cement system [10].

It is necessary to do a study that is only focused on the impact that chemically inert fillers have on the hydration of cement because there is an increasing interest in inert additives to cement, such as titanium dioxide (TiO_2). In recent years, nano-particles have garnered a lot of interest, and the different forms that they can take have proven to be highly effective in enabling the construction of concrete that is stronger, more durable, and has better mechanical properties [11].

Recently, a number of researchers [11–14] have developed cement-based or asphalt-based concrete that incorporates TiO_2 nano-particles (NT) in order to either boost the longevity of the concrete or to impart certain qualities that are desirable. There has been a significant amount of interest in the inclusion of NT into cement-based products [15]. This is because NT is environmentally friendly, has a high catalytic activity, and is inexpensive.

On the other hand, the fact that its impacts on the characteristics of cement-based materials were acknowledged was not even close to being sufficient. However, despite the fact that absorption is the primary mechanism of chloride transport in near-surface unsaturated concrete, the concentration of chlorides in this layer makes it possible for chlorides to diffuse deeper into the concrete [16]. As a consequence of this, transport of chloride ions is mostly accomplished by the process of diffusion at greater depths. Several different test protocols are available for the purpose of assessing the resistance of concrete to chloride intrusion. Each of these procedures offers either a chloride ion diffusion coefficient or an index of concrete resistance to chloride ion penetration [17].

Diffusion cells or immersion in a solution are utilized in order to evaluate the diffusivity of porous materials such as mortar. This evaluation is carried out on the assumption of steady-state chloride ion diffusion across the cement paste specimen, as stated by Fick's first law, or non-steady-state diffusion over the mortar specimen, as stated by Fick's second law [3]. When discussing the process of chloride ion diffusion in concrete, the term "non-steady state diffusion" refers to the period of time during which the ions are transported while simultaneously being attached to the cement phases. On the other hand, the term "steady state diffusion" refers to the period of time during which the flow remains constant [18]. To achieve results, however, the methods that have been recommended are time-consuming and can take several months or even years to complete, particularly in the case of high-performance concretes. The problem of being time consuming has been solved by employing an electrical field to speed up the movement of chloride ions. This has made it possible to shorten the testing period from a number of months to a few hours [19].

The resistance of concrete to penetrating chloride ions has been evaluated by the use of migration tests in a number of researches [20–22]. These tests were initially utilized to evaluate penetration based on the total penetrated load, as stated by ASTM C 1202/1992 [23], and to estimate the diffusion coefficient under steady-state conditions, as recommended by Andrade [21]. Both of these objectives were accomplished through the utilization of these tests. In recent years, a number of publications have utilized migration

studies in non-steady-state environments in order to derive the diffusion coefficient [3, 18], [24]. The process and settings of these tests may vary depending on the reason for which they are being conducted; nonetheless, they are all based on the induction of ion mobility under the influence of an external electric field [19].

Indirect correlations may exist between the results of different chloride diffusion coefficient measurements [25], even though the data from different methods cannot be directly compared. This is the case even if the findings from different methods cannot be directly compared to one another. The ionic species in the pore solution can be transported through the interconnected pore network of concrete, which follows the Nernst-Planck equation [3] as described in Eq. (1)

Nernst-Planck

Total flow = Diffusion + Migration + Convection

$$-J_j(x) = D \frac{\partial C_j(x)}{\partial x} + \frac{Z_j F}{RT} D_j C_j \frac{\partial E(x)}{\partial x} + C_j V(x)$$

1

where $J_j(x)$ is the ionic flux of species j (mol/cm²/s), D_j is the effective diffusion coefficient of species j in the concrete (cm²/s), C_j is the concentration of species j in the pore solution as a function of location x (mol/cm³), Z_j is the valence and $V(x)$ is the convection velocity of the ionic species i (cm/s), F is Faraday's constant (96487 C/mol), R is the universal gas constant (8.314 J/mol/K), T is the absolute temperature (K) and E is the electrical voltage (V). The ion movement under the concentration gradient, which is governed by Fick's first rule, the ion movement driven by the electrical potential, and the ion convection under the pressure gradient, density difference of fluid, and so on, each item in Eq. (1) has its own transportation method [4]. The concentration and pressure gradients are minimal in an electrically accelerated chloride diffusion test, and the mobility of the chloride ion is only controlled by the electrical field.

There is special case of Nernst Planck Equation, which uses electrolyte equivalent conductivity as the main parameter, which follows Nernst-Einstein [3] equation as described in Eq. (2)

Nernst-Einstein:

$$\frac{it_j}{Z_j F} = \frac{Z_j F}{RT} D_j C_j \frac{\partial E(x)}{\partial x}$$

2

where i is the current density travelling through or applied between electrodes (A/cm²), and t_j denotes the number of species transferred. In order to make both equations useful for the specific example of chloride

transport in concrete, simplifying assumptions were provided. In a typical 'diffusion cell,' the effective chloride diffusion coefficient D_{eff} was calculated using the following formulas.

Nernst–Planck:

$$D_{\text{eff}} = \frac{RTlJ_{\text{Cl}}}{\Delta EZ_{\text{Cl}}F\gamma C_{\text{Cl}}} \quad (3)$$

Where,

l is the concrete disc thickness (cm)

J_{Cl} is the chloride flow (mol/cm² per s)

γ is the activity coefficient.

Nernst–Einstein

$$D_{\text{eff}} = \frac{RT}{nF^2} \frac{it_{\text{Cl}}}{\Delta E} \frac{1}{A} \frac{1}{\gamma Z_{\text{Cl}} C_{\text{Cl}}} \quad (4)$$

Where,

t_{Cl} is the transference number of chloride ions;

A is the cross-sectional area of concrete disc (cm);

z = ion valence (chlorides = 1);

F = Faraday's constant (23063 cal/volt.eq);

R = gas constant (1.9872 cal/mol.K);

C_{Cl} = concentration of chlorides in the catholyte (mol.cm⁻³);

γ = activity coefficient of the catholyte solution (Cl⁻ = 0.657) and

ΔE = effective applied voltage (9 V)

Taguchi Method

The Taguchi method was devised by Genichi Taguchi in the 1950s as a technique for optimizing processes. The Taguchi technique of experimental design guarantees an effective, uncomplicated, and methodical approach to optimizing experimental designs for cost and performance quality. The Taguchi technique prioritizes design above the manufacturing process in quality control and aims to prevent production modifications before they occur [26–28]. Taguchi devised standard orthogonal arrays that enable the efficient evaluation of various parameters and their impact on the variability of a certain

product or process features. This can be achieved by a minimal number of tests conducted simultaneously. Subsequently, a loss function is established to calculate the discrepancies between the anticipated outcomes and the test findings. The loss function is also converted into a signal-to-noise (S/N) ratio, denoted as η [29]. Typically, there are three signal-to-noise options available, depending on the type of characteristic: higher-the-better (HB), nominal-the-better (NB), and lower-the-better (LB). When the objective of the work is to maximize a response HB is selected; when objective is to target the response NB is selected, while when aim is to minimize the response LB is selected.

In this paper, the major governing factors, which influence the effective diffusivity (D_{eff}) of chloride ions in mortar, were analyzed. These include the percentage of NT, conductivity (mS/cm) and time (in mins.) when the conductivity was measured. The NT % used in these experiments were 0, 0.5%, 1.0%, 2.0%, 2.5% and 3.0%. The values of conductivity depended on the time at which the readings were taken. This time was fixed as 0, 15 min, 30 min, 45 min, 60 min, 75 min, 90 min and 105 min. This was in accordance to the recommendations by Andrade [3]. Thus, the objectives of the current research include, obtaining the D_{eff} values for mortar containing NT in various percentages; establish the Taguchi based Grey Relational model for D_{eff} of chloride ions using three control factors, i.e., (1) NT percentage (2) time (mins.) (3) and conductivity (mS/cm) and provide Grey Relational ranking for the data. Further, the average compressive strength of mortar were investigated up to 90 days and correlation was drawn between he obtained compressive strength and the microstructure of samples at 28 days.

Experimental Method

Sample Preparation:

Cement mortars were poured into cylinder moulds measuring ϕ 25 mm by 100 mm. Three specimens were used to produce each combination. The cylinder mould was taken out after 24 hours, and all of the specimens were cured for 28 days in water at $23 \pm 2^\circ\text{C}$.

Cell type

Figure 1 shows the schematic of the cell used to calculate the diffusivity coefficient of Cl⁻ ions. This test is comparable to those recommended by ASTM C-1202 [30], AASHTO T277 [31], Nord Test NT Build 492 [20], and numerous other researchers [21], [22], [24], [32]. Over the course of the studies, a constant potential of 9 V was maintained. This is low enough to prevent unintended heating but high enough to greatly speed up the process. It is presumed that there was no voltage drop across the two chambers' liquid. 0.1 M NaCl was used in the catholyte chamber and 0.3 M NaOH in the anolyte chamber. This was in line with the recommendations made by Andrade 1994 [24] and Whiting [1]. Each chamber's solution volume remained constant at 200 millilitres. Andrade et al. [24] proposed that it is possible to achieve any solute concentration. It was also suggested that the analysis make advantage of the ions' activity.

On the other hand, diluted solutions result in low driving power and consequently contribute to inaccuracies, whereas concentrated solute solutions should not be utilized as they diminish activity [21]. However, in this instance, the 0.3M NaCl activity coefficient was 0.657.

Parameters measured

The parameters which need to be monitored during the entire process are the conductivity in the anolyte and catholyte. In order to have a comprehensive understanding of the diffusion/migration process, other parameters such as current density, chloride reduction in catholyte and both resistivity and conductivity of anolyte and catholyte were recorded. These measurements were taken at every 15 min up to 105 min.

Mortar Characteristics

Ordinary Portland cement (OPC), according to the IS 2386 – 1963(Revision 2016)[33] was used in all the tests. Standardized sand was used to prepare the mortar in the ratio 1:3 with w/b ratio as 0.46. The physical properties of cement are reported in Table 1. For each test (i.e. for 0% NT, 0.5% NT, 1% NT, 1.5% NT, 2.0 % N and 3% NT) three duplicate samples were cast and cured for 28 days at 25°C. The average values of these samples are considered in the current work. Sand conforming to Zone III and complying IS: 383–2016[34] was used. The diameter of mortar specimen taken for measurements is 2.5 cm. The length of the specimen is 5 cm for all the experiments in order to achieve non-steady state.

Table 1
Physical Properties of OPC (53 grade)

Fineness (%)	Le Chatelier Soundness (mm)	Specific Gravity	Consistency (mins.)	Setting Time (mins.)		Compressive strength (MPa)		
				IST	FST	3 Day	7 day	28 days
2.24	8.1	3.15	30	99	225	27.4	41.3	57.7

Water:

Municipally supplied portable tap water free of organic impurities, as confirmed by IS: 456–2000 [35] and IS: 10500:2012 [36], was used for mixing and curing all concrete mixes. The tap water characteristics are presented in Table 2.

Table 2
Tap water characteristics

S.No.	Parameter	Value	Unit
1	Chloride	158	mg/l
2	pH	7.3	-
3	Fluoride	0.42	mg/l
4	Dissolved Oxygen	9.18	mg/l
5	Chemical Oxygen Demand	0	-
6	Biological Oxygen Demand	0	-
7	Free Residual Chlorine	0.13	mg/l

Nano Titanium Dioxide

NT was procured from Khammam, Telangana's Nano Wings Pvt. Ltd. Based on the specifications provided by IS: 2386 Part III- 1963 [33], it was determined that the fineness modulus was 3.12. The other physiochemical features of NT that are pertinent to the discussion are listed in Table 3.

Table 3 Properties of NT			
S.No	Properties	Obtained Values	Units
1	Type	TiO ₂ (rutile)	-
2	Diameter	10–20	nm
3	pH	6.7	-
4	Surface Volume Ratio	163	m ² /g
5	Density	3.74	g/cm ³
6	Purity	> 99.9%	

Results and Discussion

In this section the average compressive strength of mortar samples on 3, 7, 28, 56 and 90 days are discussed firstly and the obtained results are correlated to the microstructure of samples. Next, a brief discussion on the diffusivity test, which includes cumulative chloride ion concentration and results of effective diffusivity, is presented. Further, based on the obtained experimental results, Taguchi Grey analysis is done.

Compressive Strength and microstructure of Mortar incorporating NT

The average compressive strength of cement mortar on 3, 7, 28, 56 and 90 days are shown in Fig. 2 with NT% varying from 0, 0.5%, 1.0%, 1.5%, 2.0%, 2.5% and 3.0% respectively. The seven days average compressive strength of cement mortar for 0, 0.5%, 1.0%, 1.5%, 2.0%, 2.5% and 3.0% of NT were 17.53, 18.67, 20.32, 22.98, 21.34, 19.64 and 15.65 MPa respectively. Similarly, at 28 days these values were 26.65, 29.11, 31.02, 33.29, 30.12, 29.10 and 24.47 MPa respectively. It is seen that as the percentage of NT increases, the compressive strength increases up to 1.5% NT then starts to decrease. Significant improvement in strength is seen from 3 to 7 days and from 7 to 28 days. After 28 days, the improvement in strength is found to reduce.

Some of the possible explanations for the increase in strength of up to 1.5% of NT include the influence of nominal pozzolanic activity of NT and the filler effect [37–39]. Both of these factors could be responsible for the improvement. The qualities of the NT also have an effect on the type of cement paste that is generated as well as the interfacial transition zone, both of which have an impact on the tensile strength of the material. Similar reasons were reported by Rawat et al.[37] which reported the compressive strength of concrete incorporating NT at similar replacement levels.

To gain a better understanding of the morphology of concrete containing NT and to provide a suitable explanation for the strength gain mechanism and to obtain a rationale for the maximum strength at 1.5% NT, micro-characterization of the mortar samples at 28 days was carried out. Hitachi S-3400N SEM, was utilized in order to investigate the microstructure. The examination of samples was conducted using a probe diameter of 2 micro-metres, an accelerating voltage of 15 kilovolts, and a probe current of 50 nano-amperes. It has been estimated that the SEM measurements result in an inaccuracy of around ± 2 at. %. The microstructure of cement mortar incorporating various percentages of NT is presented in Fig. 3 at a constant magnification of 10 μm . A homogeneous mix is seen in most part of Fig. 3(a) indicating continuous and rich C-S-H gel. This is the SEM Back-scatter image of the control mix (i.e. mix containing 0% NT).

Figure 3 (b-g) shows the SEM Back-scatter image of concrete containing 0.5%, 1.0%, 1.5%, 2.0%, 2.5% and 3.0% NT respectively. Spherical tiny particles of NT uniformly dispersed, can be clearly seen in all the images. Further, as the NT replacement increases, minute micropores can be seen. Figure 3 (d) represents the microstructure of mortar containing 1.5% NT, which appears to be dense and the pores and NT are uniformly dispersed throughout. As the NT replacement increases to 2% (Fig. 3(e)) the size of the pores increases. This increase is further more in 2.5%NT (Fig. 3(f)). At a replacement level of 3%NT (i.e. Figure 3(g)), micro-cracks are visible clearly. Based on the above discussion, it is evident that the structural behavior of the mortar is largely governed by the presence of pores and micro-cracks. The higher the pores and micro-cracks, lesser is the average compressive strength. This provides a possible explanation of 1.5%NT replacement to be the optimal value in case of cement mortar.

Cumulative Cl ion concentration in Anolyte

Figure 4 shows the total chloride concentrations in the anode cell for various mixes. It was discovered that the cumulative chloride concentration in the anode cell of three duplicate samples demonstrated good reproducibility for a given percentage of NT. When chloride reaches steady state diffusion, linear regression is used to determine the $\Delta c_a / \Delta t$ (slope). When the measured cumulative chloride concentration was more than 0.1 g/L, the steady state diffusion starting point was identified in this study [37]. Figure 4 shows the steady state diffusion starting time. Figure 4 shows a very strong association between the steady state diffusion starting time point and the percentage of NT. Because there are fewer pores in the microstructure as the percentage of NT increases, the steady state diffusion beginning time increases as well [4]. Diffusion reaches a steady state later as a result. Figure 2 shows the anode cumulative chloride concentration for the linear regression result for each of the three duplicates of each mixture. Given that the low w/c cement mortar samples have a denser bulk than the high w/c cement mortar samples, it is reasonable logical that the regression slope ($\Delta c_a / \Delta t$) declines with the reduction of w/c, indicating a lower chloride diffusion coefficient for a lower w/c cement mortar sample [37].

Diffusion test:

Figures 5 shows the averaged values of D_{eff} vs time t in anolyte and catholyte for two identical migration tests. As expected, the diffusivity coefficient values are more in control mix (typically of the order 10^{-13} cm^2/s) in case of anolyte and catholyte [27]. As the percentage of NT increases, the pores in the mortar are reduced due to the filler effect and improved microstructure thereby reducing the migration of Cl^- ions [19]. The percentage reduction of diffusivity values between control mix and mortar containing 1 %NT and 2 % NT an 1 % NT an 3 % NT at 15 min is 33.18 % and 2.14 % respectively. At the end of the experiment, i.e. at 105 min, these values are 43.82 % and 2.3 %. Also as the time increases, the effective diffusion coefficient decreases for all the samples. It is clearly seen that for samples 2% NT and 3% NT the diffusivity coefficients are significantly less, typically of the order of 10^{-14} (cm^2/s). Further, D_{eff} values for anolyte and catholyte are less upto nearly 30 min for all the samples, after which the variations are more predominant.

Optimization using Taguchi based grey relational analysis

A contemporary mathematical technique for factor analysis in a system is grey relational analysis [40, 41]. It is always employed to rank the components according to importance and assess each one's significance within a particular system. The essential idea behind it is assessing the

degree of resemblance determined by relevance calculations for a data series. Higher similarity corresponds to increased significance. GRA is used in the current research to obtain the best combination of NT (%), time (mins.) and conductivity (mS/cm) for effective diffusivity (cm^2/s).

The original dataset, D, is formed in the sequence:

$$D = \begin{bmatrix} d_1^1 & d_2^1 \cdots & d_n^1 \\ d_1^2 & d_2^2 \cdots & d_n^2 \\ \vdots & \vdots & \vdots \\ d_1^m & d_2^m \cdots & d_n^m \end{bmatrix}$$

5

Here, the original data value of the index k at solution i is represented by d_k^i . Further, the value of m in this work is 29, while the value of n is 3 (i.e. NT (%), time (mins.) and conductivity (mS/cm). The NT (%) and conductivity (mS/cm) are considered as smaller the better; while time (mins.) is considered as larger the better. Hence, the normalization is now carried out using the following equations:

$$C_k^i = \frac{d_k^i - \min(d_k^i, i = 1, 2, \dots, 29)}{\max(d_k^i, i = 1, 2, \dots, 29) - \min(d_k^i, i = 1, 2, \dots, 29)}$$

6

for larger the better response (i.e. for time) and

$$C_k^i = \frac{\max(d_k^i, i = 1, 2, \dots, 29) - d_k^i}{\max(d_k^i, i = 1, 2, \dots, 29) - \min(d_k^i, i = 1, 2, \dots, 29)}$$

7

for smaller the better response NT (%) and conductivity (mS/cm).

Thus, the C matrix is formed as below:

$$C = \begin{bmatrix} c_1^1 & c_2^1 \cdots & c_n^1 \\ c_1^2 & c_2^2 \cdots & c_n^2 \\ \vdots & \vdots & \vdots \\ c_1^m & c_2^m \cdots & c_n^m \end{bmatrix} \quad (8)$$

Next, the deviation sequence is obtained as,

$$\Delta_{0i}(k) = \|x_0^*(k) - x_i^*(k)\|$$

9

$$\Delta_{max} = \max_{max} \|x_0^*(k) - x_j^*(k)\|$$

10

$$\Delta_{min} = \min \min \| x_0^*(k) - x_j^*(k) \|$$

11

The identification coefficient ζ is considered in the range 0–1. In the present work this value is taken as 0.50. The relation between the ideal and actual normalized experimental results is finally expressed in terms of Grey relational coefficient using the formula:

$$\zeta_i(k) = \frac{\Delta_{min} + \zeta \Delta_{max}}{\Delta_{0i}(k) + \zeta \Delta_{max}}$$

12

Table 4
Taguchi Grey relational Calculations

Input			Output	Taguchi Grey Calculations				
NT %	time (min)	Conductivity (mS/cm)	Deff(cm ² /s) x 10 ⁻¹³	Deviation Sequence	Grey relational coefficient	Grey Rank	Average value of Grey Rank	Final Grey Rank
0	15	2.88	8.09	1	0.333333333	25	39	VII
0	30	2.74	7.77	0.959804	0.342511724	34		
0	45	2.57	5.04	0.6168823	0.447674746	35		
0	60	2.23	4.87	0.5955282	0.456400848	42		
0	75	2.11	3.88	0.471172	0.514841881	43		
0	90	2.09	3.41	0.4121342	0.54816498	44		
0	105	2.08	3.32	0.400829	0.555044272	47		
0.5	15	2.69	7.23	0.8919734	0.359202274	23	38	VI
0.5	30	2.51	6.16	0.7575681	0.397592768	30		
0.5	45	2.36	5.59	0.6859691	0.421596145	37		
0.5	60	2.28	4.68	0.5716619	0.466565082	41		
0.5	75	2.17	3.67	0.4447934	0.529216247	40		
0.5	90	2.11	3.45	0.4171586	0.545161953	45		
0.5	105	2.08	3.41	0.4121342	0.54816498	48		
1	15	2.61	5.87	0.7211406	0.409453274	18	34	V
1	30	2.42	5.03	0.6156262	0.448178799	27		
1	45	2.33	4.64	0.5666374	0.468762881	33		
1	60	2.21	3.99	0.4849893	0.507619716	36		
1	75	2.18	3.19	0.3844994	0.565291486	38		
1	90	2.14	3.01	0.3618892	0.580120965	39		
1	105	2.13	3	0.3606331	0.580967671	46		
1.5	15	2.57	3.88	0.471172	0.514841881	13	26	IV
1.5	30	2.46	3.03	0.3644015	0.578434934	24		
1.5	45	2.31	2.65	0.3166688	0.612243328	26		
1.5	60	2.24	2.11	0.2488381	0.667701082	28		

Input			Output	Taguchi Grey Calculations				
NT %	time (min)	Conductivity (mS/cm)	Deff(cm ² /s) x 10 ⁻¹³	Deviation Sequence	Grey relational coefficient	Grey Rank	Average value of Grey Rank	Final Grey Rank
1.5	75	2.14	1.85	0.2161789	0.69814961	29		
1.5	90	2.04	1.63	0.1885442	0.726169844	31		
1.5	105	2.01	1.61	0.1860319	0.728829076	32		
2	15	2.38	1.74	0.2023615	0.71188411	4	15	III
2	30	2.25	2.26	0.2676799	0.651313098	17		
2	45	2.19	0.647	0.0650672	0.884850506	12		
2	60	2.02	0.322	0.0242432	0.95375584	14		
2	75	1.95	0.345	0.0271323	0.948528536	16		
2	90	1.89	0.356	0.028514	0.946048723	20		
2	105	1.87	0.352	0.0280116	0.946948971	22		
2.5	15	1.89	0.363	0.0293933	0.944477399	2	11	II
2.5	30	1.74	0.649	0.0653184	0.884457283	5		
2.5	45	1.62	0.549	0.0527572	0.9045563	8		
2.5	60	1.53	0.449	0.040196	0.925590048	11		
2.5	75	1.42	0.129	0	1	10		
2.5	90	1.37	0.649	0.0653184	0.884457283	19		
2.5	105	1.32	0.641	0.0643135	0.886032276	21		
3	15	0.96	0.322	0.0242432	0.95375584	1	7	I
3	30	0.9	0.417	0.0361764	0.932528991	3		
3	45	0.67	0.647	0.0650672	0.884850506	6		
3	60	0.56	0.762	0.0795126	0.862793974	7		
3	75	0.51	0.747	0.0776284	0.865608351	9		
3	90	0.48	0.971	0.1057656	0.825401763	15		

Table 4 shows the, time and conductivity values used in the calculation of Taguchi Grey Relational ranking for various %NT replacement. The output in the calculation was effective diffusivity. The deviation sequence, Grey relational coefficient and Grey ranks are also shown in Table 4. The final ranking is

obtained based on the values of average ranks for a given NT percentage. Calculations of the grey relational coefficient are performed for every possible combination of input and output elements. Higher levels of performance are indicated by deviation sequence values that are smaller. For every possible combination, the Grey Rank and the average value of the Grey Rank are then computed. To rank the combinations, their grey relational coefficients are taken into consideration. Once the average grey rank for each NT level has been taken into consideration, the final grey rank may then be established. Generally speaking, the time, conductivity, and diffusion coefficient all decrease as the magnitude of NT increases.

At the given factors, the best performance is seen with 3% NT replacement. When it comes to time, conductivity, and diffusion coefficient, intermediate values of NT demonstrate a performance that is modest. In general, the performance of time, conductivity, and diffusion coefficient diminishes as the value of NT increases. The final grey ranks can be utilized to determine the ideal combination of input and output factors that need to be considered. In terms of performance, the lowest grey rank is related with the best performance. Taking into consideration the lower grey rankings in the final ranking, it is likely that the ideal conditions for the procedure are related with NT = 3.0% and other particular input parameters.

Conclusions

The current paper investigates the effectiveness of Nano-titania (NT) as a filler material and its impact on reducing the diffusivity (D_{eff}) of chloride ions in mortar. The concentration of NT in the material influences the flow of Cl^- ions or flux through the mortar, resulting in a decrease with increasing NT content, indicating a delay in ion migration. Increasing the amount of NT correlates with a decrease in the diffusion of Cl^- ions in the anolyte chamber, with the control specimen exhibiting the highest diffusion. The diffusion of Cl^- ions in the NT-containing sample is significantly lower than in the control sample, signifying a decrease in Cl^- ion mobility in both chambers. A Taguchi-based grey relational analysis method was used to determine the ideal parameters that will reduce the effective diffusivity in mortar containing NT. Based on this study, optimal D_{eff} was obtained at 2% NT replacements. The Grey ranking suggested poorest ranks of D_{eff} for control mix. Grey relational coefficients and rankings quantify the input-output relationship. This study could improve process efficiency by determining grey relational coefficients which in turn affects the resource use, energy efficiency, and cost-effectiveness. Taguchi Grey relational analysis gives a quantitative and rigorous way to analyze varied relationships. This research could be used to a variety of fields of civil engineering that use similar approaches or systems. Engineers, scientists, and practitioners seeking to improve analogous processes may find the insights beneficial.

Declarations

Conflict of Interest

The author declares that they have no conflict of interest.

Funding

This research did not receive any specific grant from funding agencies in the public, commercial, or not-for-profit sectors.

Author Contribution

YIM prepared the entire paper and is the sole author

Acknowledgement

The author is thankful to the Department of Civil Engineering at JUET, Guna, India, for all the support.

Data availability

The data that support the findings of this study are available from the corresponding author upon reasonable request.

References

1. Whiting, D. (1981). Rapid Determination of the Chloride Permeability of Concrete, [Online]. Available: <https://www.fhwa.dot.gov/publications/publicroads/>.
2. Tang, L., & Nilsson, L. O. (1992). Chloride Diffusivity in High Strength Concrete, *Nordic Concrete Research*, vol. 11, no. August, pp. 162–170.
3. Andrade, C. (2005). Concepts on the chloride diffusion coefficient. *no September*. 10.1617/2912143578.001.
4. Dhir, R. K., Jones, M. R., Ahmed, H. E. H., Seneviratne, A. M. G., Buenfeld, N. R., & El-Belbol, S. (1991). Rapid estimation of chloride diffusion coefficient in concrete. *Magazine of Concrete Research*, 43(155), 135–139. 10.1680/mac.1991.43.155.135.
5. Lee, B. Y., & Kurtis, K. E. (2010). Influence of TiO₂ nanoparticles on early C3S hydration. *Journal of the American Ceramic Society*, 93(10), 3399–3405. 10.1111/j.1551-2916.2010.03868.x.
6. Chen, J., Kou, S. C., & Poon, C. S. (2012). Hydration and properties of nano-TiO₂ blended cement composites. *Cement and Concrete Composites*, 34(5), 642–649. 10.1016/j.cemconcomp.2012.02.009.
7. Jayapalan, A. R., Lee, B. Y., & Kurtis, K. E. (2009). Effect of Nano-sized Titanium Dioxide on Early Age Hydration of Portland Cement. *Nanotechnology in Construction*, 3, 267–273. 10.1007/978-3-642-00980-8_35.
8. Zhang, R., Cheng, X., Hou, P., & Ye, Z. (2015). Influences of nano-TiO₂ on the properties of cement-based materials: Hydration and drying shrinkage. *Construction and Building Materials*, 81, 35–41.

- 10.1016/j.conbuildmat.2015.02.003.
9. Du, S., Wu, J., Alshareedah, O., & Shi, X. (2019). Nanotechnology in cement-based materials: A review of durability, modeling, and advanced characterization. *Nanomaterials*, 9(9). 10.3390/nano9091213.
 10. Saloma, A., Nasution, I., Imran, & Abdullah, M. (2015). Improvement of concrete durability by nanomaterials. *Procedia Engineering*, 125, 608–612. 10.1016/j.proeng.2015.11.078.
 11. Jalal, M. (2012). Durability enhancement of concrete by incorporating titanium dioxide nanopowder into binder. *Journal of American Science*, 8(4), 289–294.
 12. Shekari, A. H., & Razzaghi, M. S. (2011). Influence of nano particles on durability and mechanical properties of high performance concrete. *Procedia Engineering*, 14, 3036–3041. 10.1016/j.proeng.2011.07.382.
 13. Mohseni, E., Naseri, F., Amjadi, R., Khotbehsara, M. M., & Ranjbar, M. M. (2019). Microstructure and durability properties of cement mortars containing nano-TiO₂ and rice husk ash, *Construction and Building Materials*, vol. 114, no. February pp. 656–664, 2016, 10.1016/j.conbuildmat.2016.03.136.
 14. Ma, B., Li, H., Mei, J., Li, X., & Chen, F. (2015). Effects of nano-TiO₂ on the toughness and durability of cement-based material, *Advances in Materials Science and Engineering*, vol. 2015, 10.1155/2015/583106.
 15. Yu, X., Kang, S., & Long, X. (2036). Compressive strength of concrete reinforced by TiO₂ nanoparticles, *AIP Conference Proceedings*, vol. no. November, pp. 2–7, 2018, 10.1063/1.5075659.
 16. Luna, F. J., Fernández, & Alonso, M. C. (2018). The influence of curing and aging on chloride transport through ternary blended cement concrete. *Materiales de Construccion*, 68(332). 10.3989/mc.2018.11917.
 17. Jayapalan, A. R., Lee, B. Y., Fredrich, S. M., & Kurtis, K. E. (2010). Influence of additions of anatase TiO₂ nanoparticles on early-age properties of cement-based materials. *Transportation Research Record*, 2(2141), 41–46. 10.3141/2141-08.
 18. Zeng, L., & Song, R. (2013). Controlling chloride ions diffusion in concrete. *Scientific Reports*, 3, 1–7. 10.1038/srep03359.
 19. Song, L., Sun, W., & Gao, J. (2013). Time dependent chloride diffusion coefficient in concrete. *Journal Wuhan University of Technology Materials Science Edition*, 28(2), 314–319. 10.1007/s11595-013-0685-6.
 20. 492, N. T. B. (1999). Concrete, mortar and cement-based repair materials: Chloride migration coefficient from non-steady-state migration experiments. *Measurement*, pp. 1–8.
 21. Andrade, C. (1993). Calculation of chloride diffusion coefficients in concrete from ionic migration measurements. *Cement and Concrete Research*, 23(3), 724–742. 10.1016/0008-8846(93)90023-3.
 22. Nakamura, E., Suzuki, S., & Watanabe, H. (2013). Non-steady-state chloride migration test on mortar with supplementary cementitious materials. *Sustainable Construction Materials and Technologies 2013-Augus*.
 23. ASTM C1202 (2012). Standard Test Method for Electrical Indication of Concrete's Ability to Resist Chloride Ion Penetration, American Society for Testing and Materials., no. C, pp. 1–8, 10.1520/C1202-

12.2.

24. Andrade, C., & Sanjuán, M. A. (1994). Experimental procedure for the calculation of chloride diffusion coefficients in concrete from migration tests, *Advances in Cement Research*, vol. 6, no. 23, pp. 127–134, 10.1680/adcr.1994.6.23.127.
25. Sakai, Y. (2019). Relationship between pore structure and chloride diffusion in cementitious materials, *Construction and Building Materials*, vol. 229, no. December, pp. 1–14, 10.1016/j.conbuildmat.2019.116868.
26. Gailius, A., & Kosior-Kazberuk, M. (2008). Monitoring of concrete resistance to chloride penetration. *Medziagotyra*, 14(4), 350–355.
27. Liu, Y., Presuel-Moreno, F. J., & Paredes, M. A. (2015). Determination of chloride diffusion coefficients in concrete by electrical resistivity method. *ACI Materials Journal*, 112(5), 631–640. 10.14359/51687777.
28. Layssi, H., Ghods, P., Alizadeh, A. R., & Salehi, M. (2015). Electrical Resistivity of Concrete: Concepts, applications, and measurement techniques, *Concrete International*, no. May, pp. 41–46.
29. Li, H., Xiao, H., Guan, X., Wang, Z., & Yu, L. (2014). Chloride diffusion in concrete containing nano-TiO₂ under coupled effect of scouring. *Composites Part B: Engineering*, 56, 698–704. 10.1016/j.compositesb.2013.09.024.
30. ASTM T277. (2000). Electrical indication of concrete's ability to resist chloride ion penetration. *ASTM International*, C0402(18), 21–27.
31. Ribeiro, D. V., Labrincha, J. A., & Morelli, M. R. (2011). Chloride diffusivity in red mud-ordinary portland cement concrete determined by migration tests. *Materials Research*, 14(2), 227–234. 10.1590/S1516-14392011005000026.
32. Bureau of Indian Standards Bureau of Indian Standards, 'IS: 2386 – 1963,' Indian Stand. methods test aggregates Concr. (Part-I to Part-VIII). Revision 2016, Bureau of Indian Standards.
33. Bureau of Indian Standards (Revision 2016). IS 2386 – 1963 Part III, Method of Test for aggregate for concrete. Part III- Specific gravity, density, voids, absorption and bulking, Bureau of Indian Standards, New Delhi, 2016.
34. Bureau of Indian Standards, IS 383 (1970). 2016 Specification for Coarse and Fine Aggregates From Natural Sources for Concrete. *Indian Standards*, pp. 1–24.
35. Bureau of Indian, & Standards (2000). IS 456:2000, Plain and Reinforced Concrete - Code of Practice (Fourth Revision), Bureau of Indian Standards, New Delhi, India, no. July, p. New Delhi,India.
36. Bureau of Indian Standards (2012). IS: 10500:2012, Indian Standard for drinking water. New Delhi, India, no. July, p. New Delhi,India.
37. Rawat, G., Gandhi, S., & Murthy, Y. I. (2022). Influence of nano-TiO₂ on the chloride diffusivity of concrete. *Emerging Materials Research*, 11(4), 495–505.
38. Rawat, G., Gandhi, S., & Murthy, Y. I. (2023). Durability Aspects of Concrete Containing Nano-Titanium Dioxide. *ACI Materials Journal*, 120(2), 25–35.

39. Rawat, G., Gandhi, S., & Murthy, Y. I. (2022). Strength and rheological aspects of concrete containing nano-titanium dioxide. *Asian Journal of Civil Engineering*, 23(8), 1197–1208.
40. Chen, J., Wang, J., He, R., Shu, H., & Fu, C. (2021). Experimental study on effective chloride diffusion coefficient of cement mortar by different electrical accelerated measurements. *Crystals (Basel)*, 11(3), 1–13. 10.3390/cryst11030240.
41. Keleştemur, O., Arıcı, E., Yıldız, S., & Gökçer, B. (2014). Performance evaluation of cement mortars containing marble dust and glass fiber exposed to high temperature by using Taguchi method. *Construction And Building Materials*, 60, 17–24.

Figures

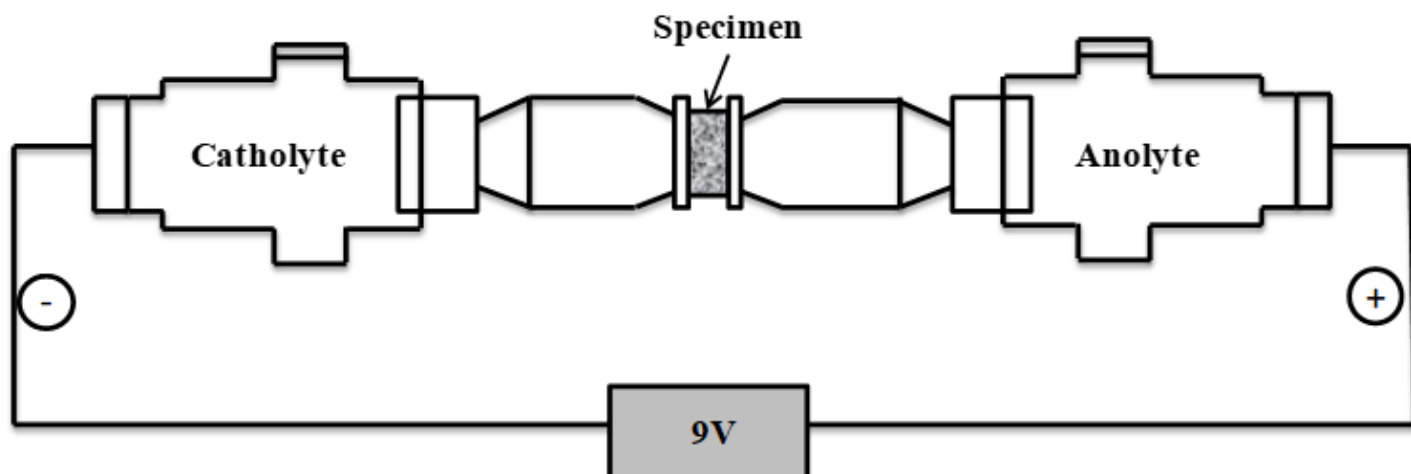


Figure 1

Layout of the chloride migration test

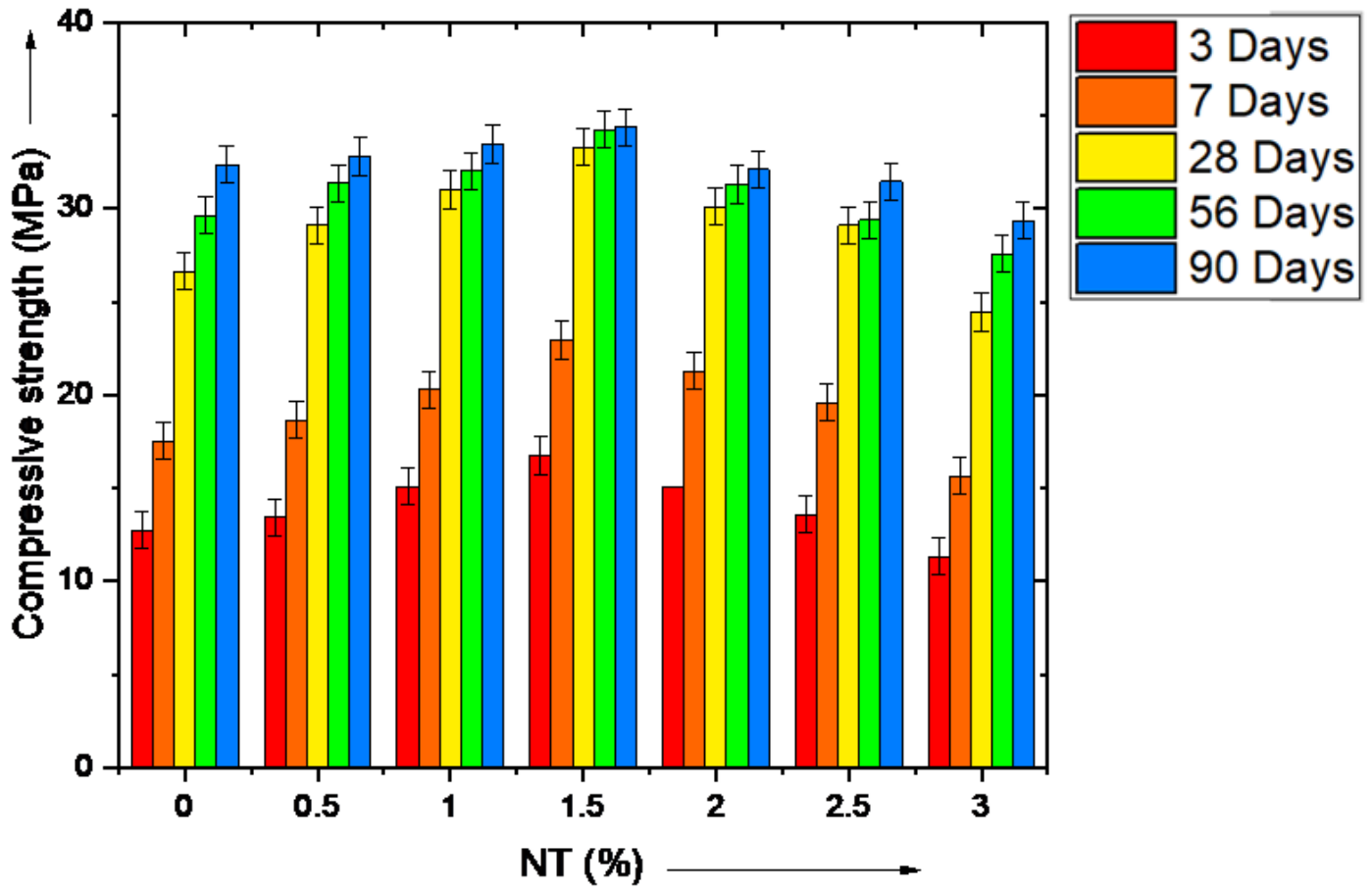


Figure 2

Compressive strength values for cement mortar incorporating NT for various days

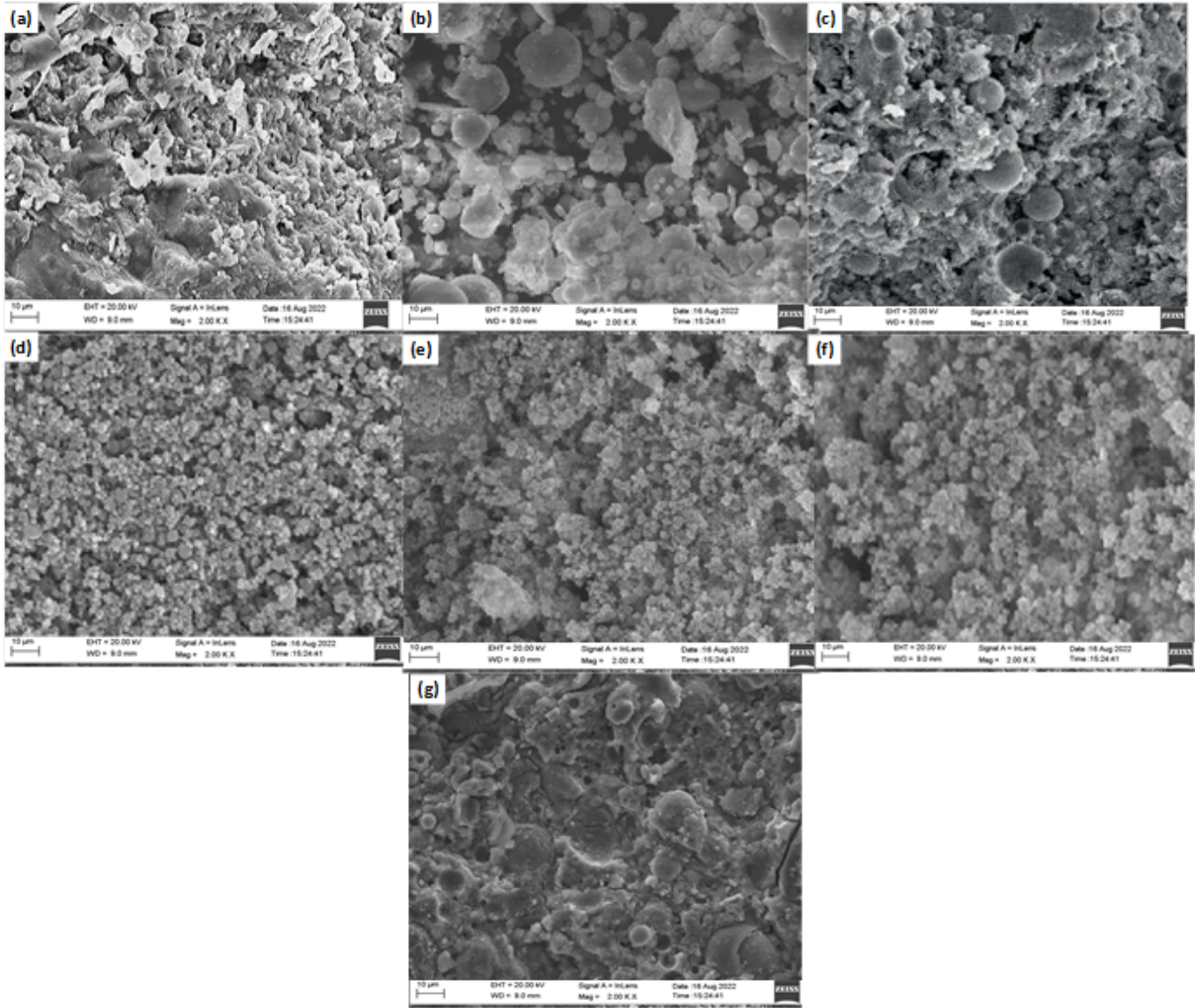


Figure 3

Micro-structure of cement mortar incorporating NT for various NT%

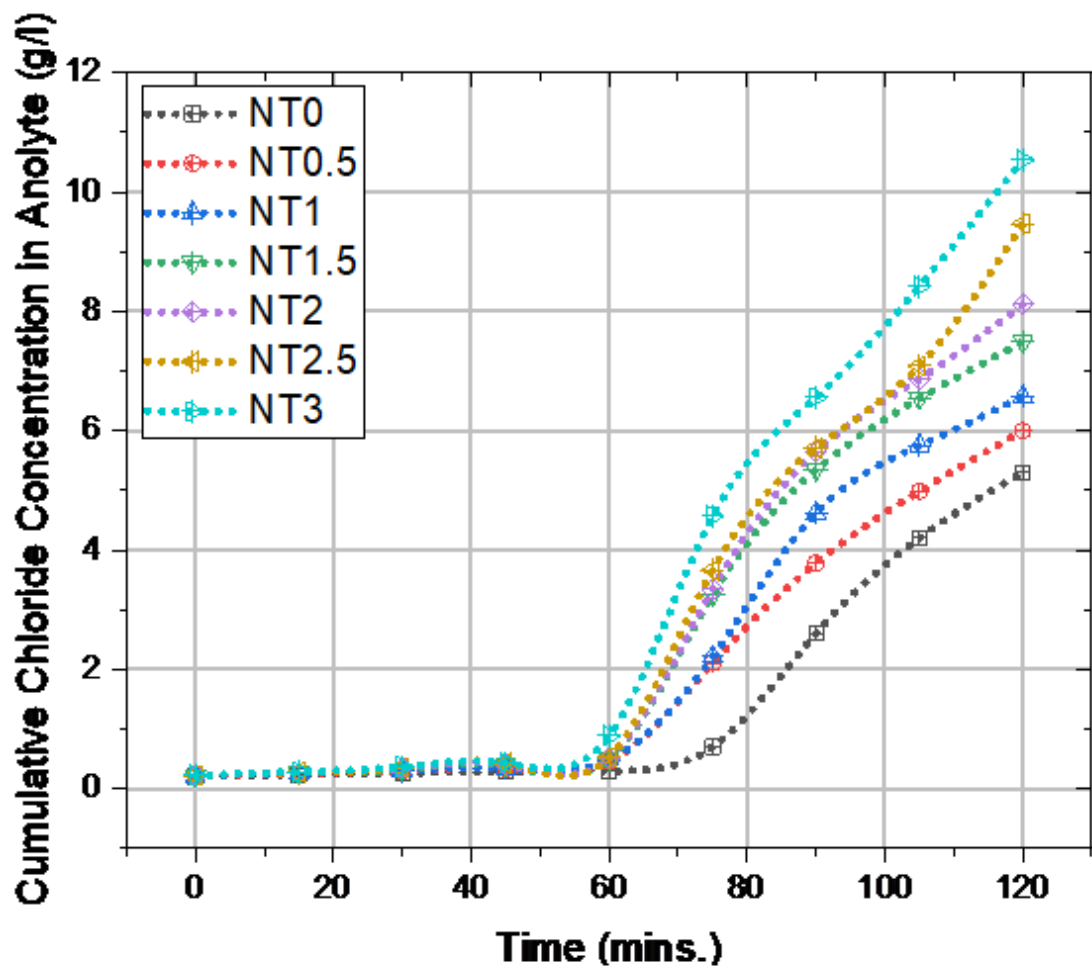


Figure 4

Total chloride concentrations in the anode cell

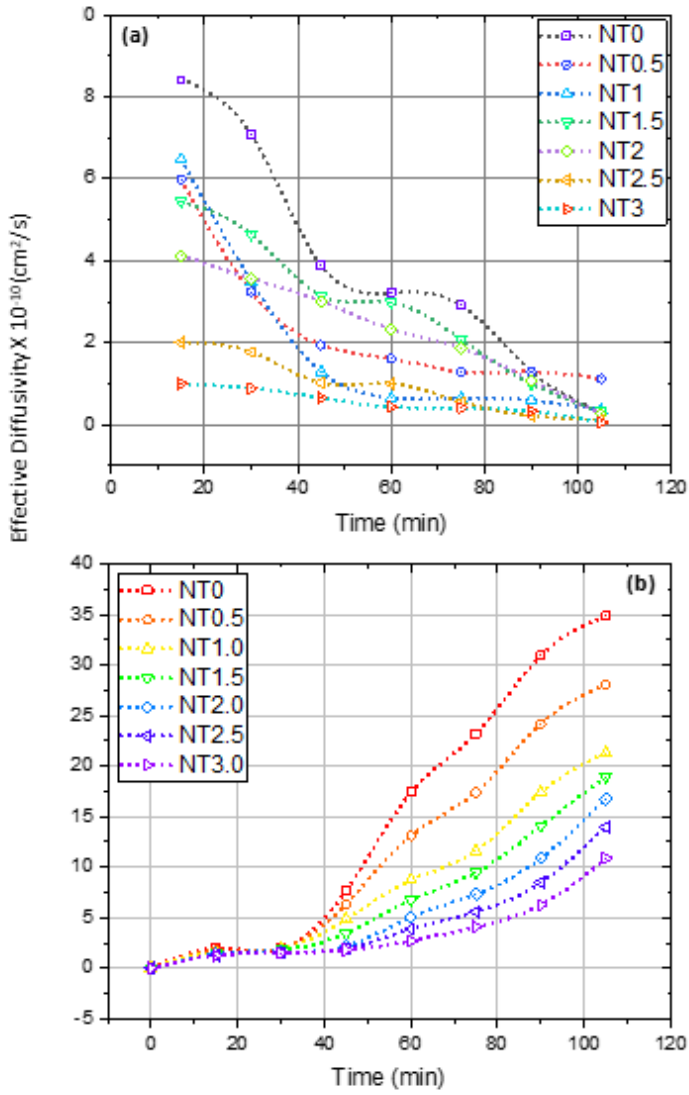


Figure 5

Plot of Diffusivity coefficient vs time for duplicate experiments for (a) Analyte and (b) Catholyte